HOT-WORKABILITY OF INCONEL 600 AND HASTELLOY X

M. SAKAKIBARA AND S. SEKINO

Technical Research Inst., Yawata Works,
Nippon Steel Corp. Kitakyushu, Japan

SYNOPSIS

The hot-workability of Inconel 600 and Hastelloy X was investigated, varying the melting practices, minor elements, impurities. It was clarified that it was improved by decreasing Cu and Mn content, by adding B, Be, Zr and Ce, by decreasing inclusions, and by decreasing γ grain size. The effective processes for its improvement were electro-slag remelting, refining under vacuum, diffusion-annealing, and increase of forging ratio.

I INTRODUCTION

Superalloys are widely used because of their excellent properties at high temperature and in corrosive atmospheres. But there are many problems in the production as they have generally poor workability. To expand their uses to larger and longer products, it is necessary to improve the hot-workability. The factors which control the hot-workability, seem to be the ductility of alloys themselves, the strength of γ grain boundaries(1), inclusions(2), precipitates, segregations(3), and impurities which generally relate intimately to grain boundaries. These factors depend upon the chemical composition, casting conditions, deformation conditions and heat-treatments etc. We examined in this report, the effect of production processes on the hot-workability of Inconel 600 and Hastelloy X.

II EXPERIMENTAL PROCEDURES

Although it is not widely accepted that the torsion test is the best one to estimate quantitively the hot-workability, we adopted it and also forging test. In forging test, $\frac{1}{4}$ t hammer was used and the workability was estimated by the degree of cracking in the temperature range 1000° - 1300°C. In torsion test, the specimen shown in Fig.1 was kept at test temperatures for 30 min, and then revolved with the speed of 100 rpm until break.

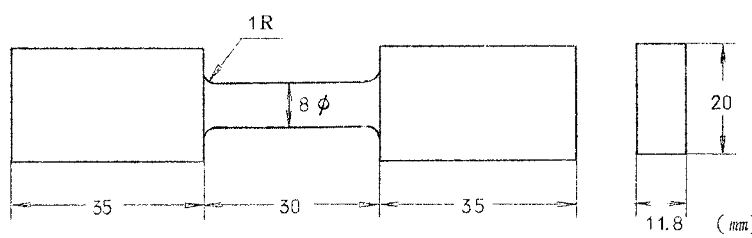

Fig.1. Size of specimen for hot-torsion test.

Samples were melted by 250 kg electric arc furnace in open air(AM), by 20 and 100 kg vacuum induction furnaces(VIM), 50 kg vacuum arc remelting furnace(VAR), 50 kg electro-slag remelting furnace(ESR). In VIM, the alloys were refined at 1550°-1700°C for 20 - 180 min under the vacuum pressure of 1 - 10^{-4} mmHg.

III EXPERIMENTAL RESULTS AND DISCUSSIONS

Table 1 shows the chemical composition of samples. A - Y are Inconel 600 and HA - HL are Hastelloy X. Sample A was made by 250 kg AM, B by ESR from row material A, C by 100 kg VIM, D and E by VAR and ESR from row material C, F - O by VIM so as to examine the refining conditions ___ temperature, time and vacuum, P - X made by 20 kg VIM so as to examine the effect of alloying elements such as B, Be, Zr, and Ce etc.

1. Effect of melting practices on the hot-workability

Fig.2 shows the relation between hot-workability and melting practices. These alloys had almost the same chemical composition and showed rather poorer hot-workabil-

Table 1. Chemical composition of specimens

Alloy		C	Si	Mn	Ni	Cr	Cu	Fe	Ti	Al	Co	Mo	W	Others	Remarks
INCONEL 600	A	0.03	0.20	0.30	67.0	15.8	0.10	16.5	0.48	0.40	NO ADD	NO ADD	NO ADD		AM *1
	B	0.02	0.14	0.25	71.8	14.1	0.11	11.8	0.41	0.43	NO ADD	NO ADD	NO ADD		AM-ESR
	C	0.03	0.20	0.24	70.0	17.0	0.10	11.3	0.47	0.40	NO ADD	NO ADD	NO ADD		VIM
	D	0.03	0.20	0.20	75.0	15.5	0.10	7.2	0.40	0.40	NO ADD	NO ADD	NO ADD		VIM-VAR
	E	0.03	0.20	0.20	75.0	15.5	0.10	7.2	0.40	0.40	NO ADD	NO ADD	NO ADD		VIM-ESR
	F	0.006	0.20	0.065	77.0	13.7	0.066	7.7	NO ADD	NO ADD	NO ADD	NO ADD	NO ADD		*2 $1550^{\circ}C \times 60' \times 10^{-4}$
	G	0.002	0.18	0.020	77.8	12.7	0.022	7.8	NO ADD	NO ADD	NO ADD	NO ADD	NO ADD		$1550^{\circ}C \times 180' \times 10^{-4}$
	H	0.002	0.19	0.150	77.8	14.1	0.086	7.2	NO ADD	NO ADD	NO ADD	NO ADD	NO ADD		$1625^{\circ}C \times 60' \times 10^{0}$
	I	0.002	0.19	0.038	76.5	13.6	0.047	6.9	NO ADD	NO ADD	NO ADD	NO ADD	NO ADD		$1625^{\circ}C \times 60' \times 10^{-2}$
	J	0.002	0.21	0.025	77.0	13.1	0.037	6.9	NO ADD	NO ADD	NO ADD	NO ADD	NO ADD		$1625^{\circ}C \times 60' \times 10^{-4}$
	K	0.001	0.18	0.016	75.0	12.8	0.018	7.5	NO ADD	NO ADD	NO ADD	NO ADD	NO ADD		$1625^{\circ}C \times 180' \times 10^{-4}$
	L	0.003	0.18	0.030	75.7	13.2	0.044	7.0	NO ADD	NO ADD	NO ADD	NO ADD	NO ADD		$1700^{\circ}C \times 20' \times 10^{-4}$
	M	0.001	0.20	0.095	77.0	13.7	0.069	6.5	NO ADD	NO ADD	NO ADD	NO ADD	NO ADD		$1700^{\circ}C \times 60' \times 10^{0}$
	N	0.002	0.16	0.005	76.5	12.5	0.013	7.0	NO ADD	NO ADD	NO ADD	NO ADD	NO ADD		$1700^{\circ}C \times 60' \times 10^{-4}$
	O	0.001	0.14	0.006	74.0	11.7	0.009	7.1	NO ADD	NO ADD	NO ADD	NO ADD	NO ADD		$1700^{\circ}C \times 180' \times 10^{-4}$
	P	0.03	0.07	0.07	75.5	15.5	ND	8.0	0.40	0.40	NO ADD	NO ADD	NO ADD	0.002B	VIM
	Q	0.03	0.07	0.07	75.5	15.5	ND	8.0	0.40	0.40	NO ADD	NO ADD	NO ADD	0.007B	VIM
	R	0.03	0.07	0.07	75.5	15.5	ND	8.0	0.40	0.40	NO ADD	NO ADD	NO ADD	0.02Be	VIM
	S	0.03	0.07	0.07	75.5	15.5	ND	8.0	0.40	0.40	NO ADD	NO ADD	NO ADD	0.07Be	VIM
	T	0.03	0.07	0.07	75.5	15.5	ND	8.0	0.40	0.40	NO ADD	NO ADD	NO ADD	0.02Zr	VIM
	U	0.03	0.07	0.07	75.5	15.5	ND	8.0	0.40	0.40	NO ADD	NO ADD	NO ADD	0.07Zr	VIM
	V	0.03	0.07	0.07	75.5	15.5	ND	8.0	0.40	0.40	NO ADD	NO ADD	NO ADD	0.007B-0.07Be	VIM
	W	0.03	0.07	0.07	75.5	15.5	ND	8.0	0.40	0.40	NO ADD	NO ADD	NO ADD	0.007B-0.07Zr	VIM
	X	0.03	0.07	0.07	75.5	15.5	ND	8.0	0.40	0.40	NO ADD	NO ADD	NO ADD	0.007B-0.07Ce	VIM
	Y	0.04	0.15	0.03	75.5	15.5	$<$0.01	6.8	0.40	0.40	NO ADD	NO ADD	NO ADD	—	AM
HASTE-LLOY-X	HA	0.07	0.26	0.75	Bal	21.0	ND	19.4	NO ADD	NO ADD	1.3	8.3	0.7	0.003B	VIM
	HB	0.07	0.26	0.75	Bal	21.0	ND	19.4	NO ADD	NO ADD	1.3	8.3	0.7	0.007B	VIM
	HC	0.07	0.26	0.75	Bal	21.0	ND	19.4	NO ADD	NO ADD	1.3	8.3	0.7	0.003B-0.03Be	VIM
	HD	0.07	0.26	0.75	Bal	21.0	ND	19.4	NO ADD	NO ADD	1.3	8.3	0.7	0.003B-0.08Be	VIM
	HE	0.07	0.26	0.75	Bal	21.0	ND	19.4	NO ADD	NO ADD	1.3	8.3	0.7	0.003B-0.035Zr	VIM
	HF	0.07	0.26	0.75	Bal	21.0	ND	19.4	NO ADD	NO ADD	1.3	8.3	0.7	0.003B-0.09Zr	VIM
	HG	0.07	0.26	0.75	Bal	21.0	ND	19.4	NO ADD	NO ADD	1.3	8.3	0.7	0.003B-0.035Ce	VIM
	HH	0.07	0.26	0.75	Bal	21.0	ND	19.4	NO ADD	NO ADD	1.3	8.3	0.7	0.003B-0.09Ce	VIM
	HI	0.07	0.26	0.75	Bal	21.0	ND	19.4	NO ADD	NO ADD	1.3	8.3	0.7	0.003B-0.035Zr -0.03Be	VIM
	HJ	0.07	0.26	0.75	Bal	21.0	ND	19.4	NO ADD	NO ADD	1.3	8.3	0.7	0.003B-0.035Ce -0.03Be	VIM
	HK	0.07	0.26	0.75	Bal	21.0	ND	19.4	NO ADD	NO ADD	1.3	8.3	0.7	0.003B-0.035Ce -0.035Zr	VIM
	HL	0.07	0.26	0.75	Bal	21.0	ND	19.4	NO ADD	NO ADD	1.3	8.3	0.7	0.003B-0.035Ce 0.03Be-0.035Zr	VIM

*1 AM: AIR-MELTING, VIM: VACUUM MELTING, VAR: VACUUM-ACR REMELTING,

*2 TEMPERATURE, TIME, AND DEGREE OF VACUUM IN VACUUM REFINING.

ity. This fact may be explained by the higher content of Cu, Mn and Fe as explained later. The increase of hot-workability of alloys made by VAR and ESR may by explained by the finer casting structure because of their higher cooling rate and the decrease of P and S as indicated by Kelley (4).

2. Effect of vacuum melting conditions

Fig.3 shows the effect of the refining temperature and time on the hot-workability under the vacuum pressure of 10^{-4} mmHg. Fig.4 shows the effect of vacuum pressure at refining conditions of 1625°, 1700°C for 60 min. The higher the refining temperature, the longer the refining time and the higher the vacuum, the better the hot-workability. This fact may be explained by the decrease of some detrimental elements by vaporization, gas components and inclusions. Under vacuum, C, Mn, and Cu decreased much, and other elements such as Si, P, S, Ni, Fe, N, H, As, Sb, Sn, and O changed little. Fig.5 shows the effect of Cu plus Mn on the hot-workability which decreased as Cu and Mn increased. In the course of forging, the materials containing higher Cu and Mn, cracked on the surface and at the corner of forged ingots. All cracks were along γ grain boundaries. Fig.6 shows the results of EPMA analysis of the extreme of a crack. It was ascertained that Cu and Mn segregated on γ grain boundaries. The segregation may be the reason of the poorer hot-workability. It could be decreased by the diffusion-annealing as explained later.

Fig.7 shows the effect of inclusions on the number of revolutions in Inconel 600 and Hastelloy X. In Inconel 600, the number increased as the inclusion content decreased, but in Hastelloy X this relation was not clear, perhaps because of the too low level of hot-workability. In both alloys, the inclusions were round, Si-rich and type categoly C. Fig.8 shows the effect of oxygen content on the hot-workability in Inconel 600, where no clear relation was observed.

Fig.9 shows the effect of Si. As Si content decreased, the inclusion

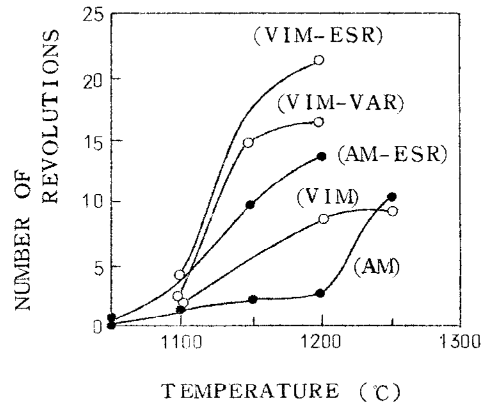

Fig.2. Effect of melting practices on the hot-workability in Inconel 600.

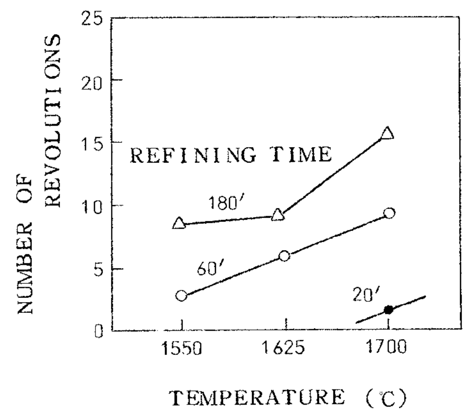

Fig.3. Effect of refining temperature, time under 10^{-4} mmHg on the hot-workability in Inconel 600.

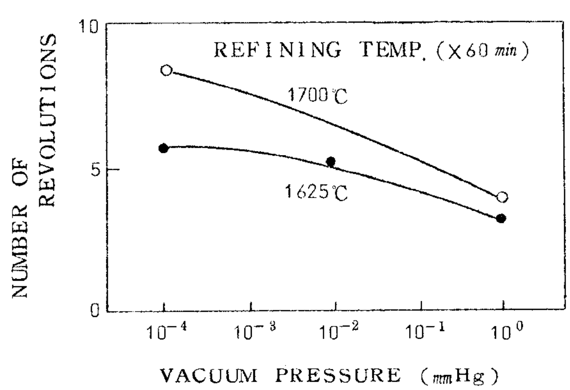

Fig.4. Effect of vacuum pressure during vacuum refining on the hot-workability in Inconel 600.

content decreased and the hot-workability increased. From the above experimental results, it can be said that the detrimental elements to hot-workability were Cu, Mn, of which effect was through grain boundaries, and Si, through inclusions. Savage et al. indicated also harmful effect of Mn and Si(5).

Next, will be discussed the effect of casting structure and γ grain size on the hot- workability. In the as-cast condition, as Fig.10 shows, alloys almost broke along the primary γ grain boundaries, so that alloys having the finest macro-structure showed the highest hot-workability. Fig.11 shows the macro-structures of alloys made by different melting practices.

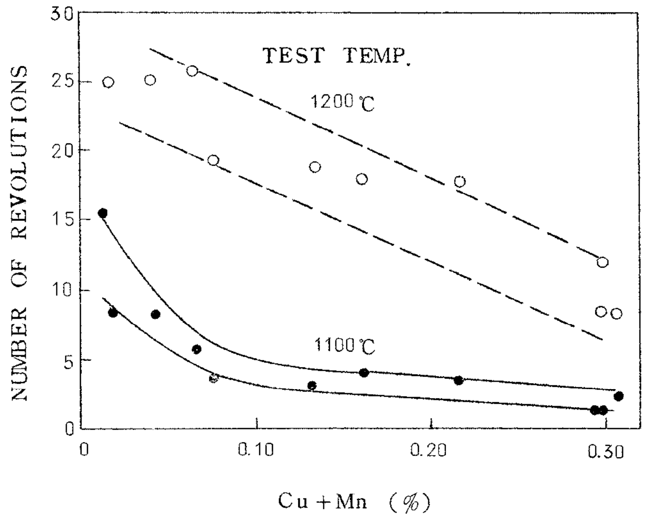

Fig.5. Effect of Cu and Mn content on the hot-workability in Inconel 600 made by VIM.

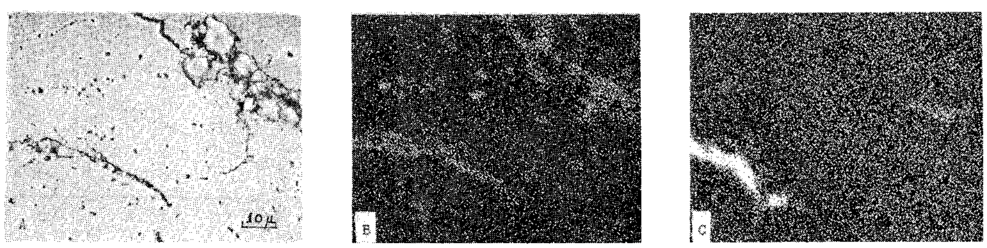

Fig.6. Elemental X-ray images of the extreme of crack in forged Inconel 600.

A: Sample current B: S-Kα

C: Mn-Kα

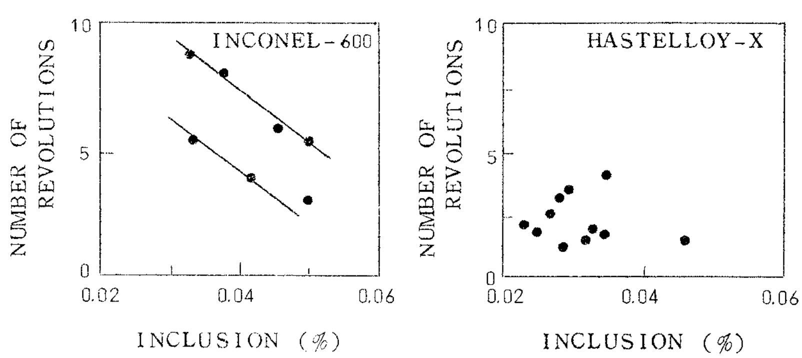

Fig.7. Effect of inclusion content on the hot-workability at 1100°C in Inconel 600 and Hastelloy X made by VIM.

It may be pointed out that ESR was the best process in this regard. One primary γ grain is divided into several sub-grains. Fig.12-(a) shows the relation between the surface area of sub-grain boundaries and the hot-workability. The correlation is not clear if the points of fine primary γ grains are omitted. Hence it can be said that the sub-grain size is not important for the hot-workability. The segregation on boundaries can be detected by EPMA. There were highly segregated boundaries and less segregated ones. The former may correspond to the primary γ grain boundaries.

After forging, γ grains become much finer and the relation between the surface area of γ grain boundaries and the hot-workability is clearly recognized as shown in Fig.12-(b). In this case, the weak planes in as-cast condition —— the primary γ grain boundaries where the detrimental elements segregate much during solidification —— may be smothered, and γ grain boundaries produced by recrystallization become instead the weakest planes.

Fig.13 shows the cross section of fractured surface of forged-specimens having coarse or fine grains. In the coarse grain size specimen, there was observed almost no deformation of γ grains, on the other hand in the small grain size specimen, the grain were fairly deformed before cracking.

Perhaps one of reasons may be the fine grain specimen has higher elongation at high temperature. Anyhow, both specimens broke out along the γ grain boundaries.

3. Effect of minor elements

As explained already, grain boundaries had a decisive influence on the hot-workability. Fig.14-(a) and (b) show the hot-workability of Inconel 600 and Hastelloy X, when at least one of B, Zr, and Ce was added as minor elements. In every alloy to which B, Be and/or Zr were added, the hot-workability was improved. Especially the combination of Ce-Be-Zr was effective. It may be very difficult to clarify the real function of these elements. R.F. Decker et al. pointed out that B and Zr impede the

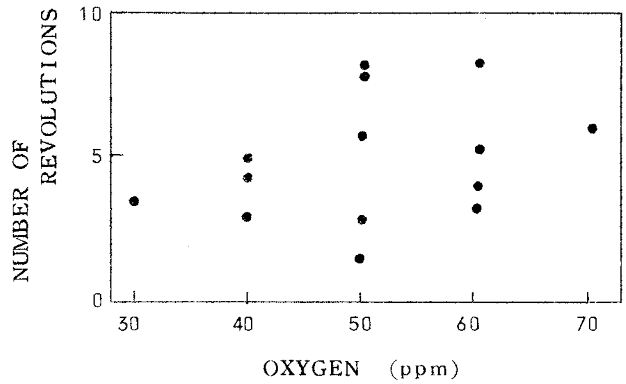

Fig.8. Effect of oxygen content on the hot-workability at 1100°C in Inconel 600 made by VIM.

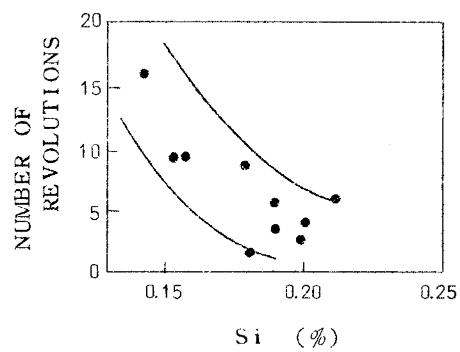

Fig.9. Effect of Si content on the hot-workability in Inconel 600 made by VIM.

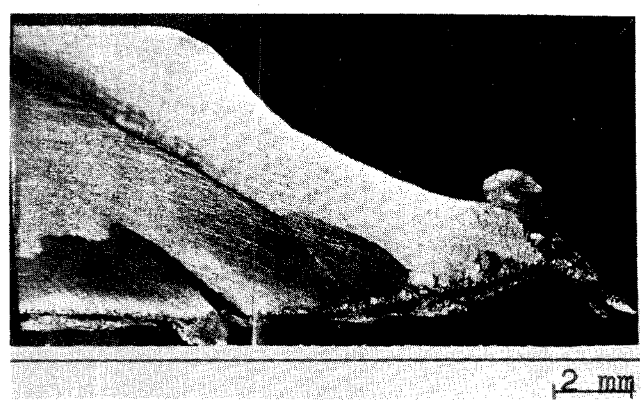

Fig.10. Cross section of a fractured specimen. Cracks were observed, propagating along the primary grain boundaries.

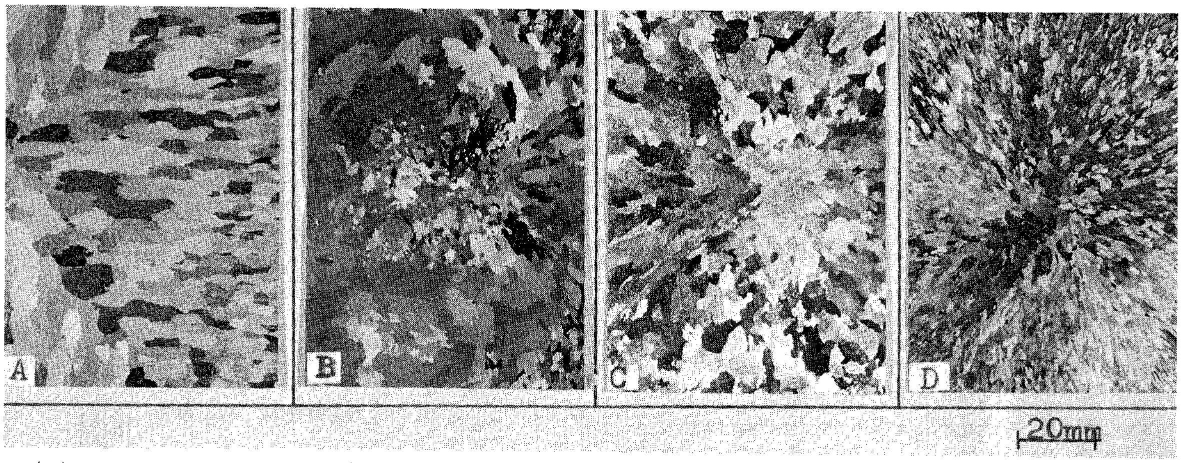

(a) AM (b) VIM (c) VAR (d) ESR

Fig.11. Effect of melting practices on macro-structures.

segregation of detrimental elements on grain boundaries (6). Fig.15 shows the distribution of B disclosed by fission track method in as-cast condition of Inconel 600 in the case of B, B-Be and B-Zr additions. In these photographs, the segregation of B on grain boundaries or sometimes on sub-grain boundaries is clearly recognized, especially in B-Zr added alloy, which showed the best hot-workability.

4. Diffusion-annealing and hot-workability

As already indicated, the segregation on grain boundaries seems to control the hot-workability, so that the diffusion-annealing which makes segregated impurities diffuse into grains, may be effective to the improvement of hot-workability. Fig.16 shows the effect of diffusion-annealing on the hot-workability in Inconel 600. As the annealing time increased, the segregation decreased as shown in Fig.17, and the hot-workability was also improved.

Fig.18 shows the torsion test result of air-melted Inconel 600 having the improved chemical composition —— low Si, Mn and Cu.

IV CONCLUSIONS

The factors which control the hot-workability of Inconel 600 and Hastelloy X were investigated and it was clarified that the following factors improved the

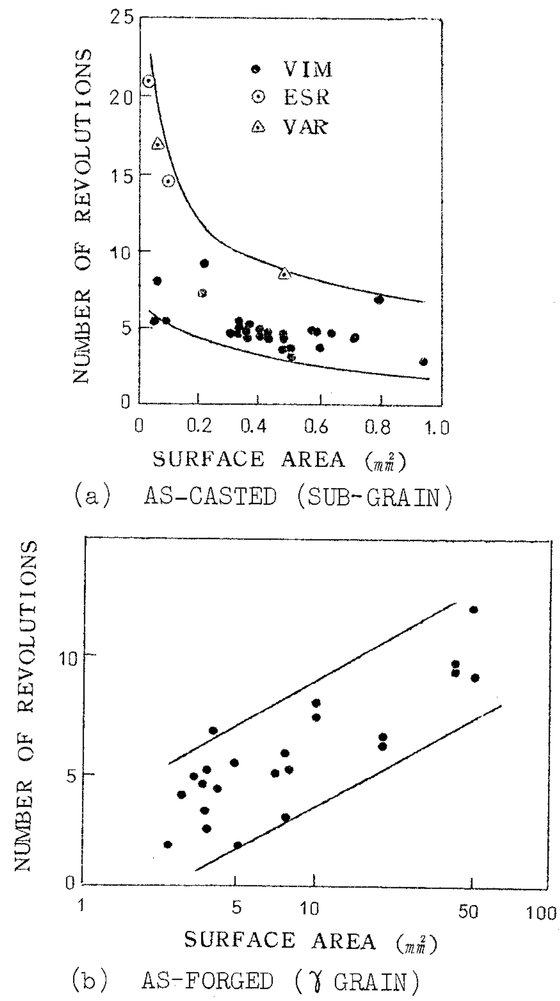

Fig.12. Effect of the total surface area of grain boundaries in the unit volume on the hot-workability at 1200°C in Inconel 600.

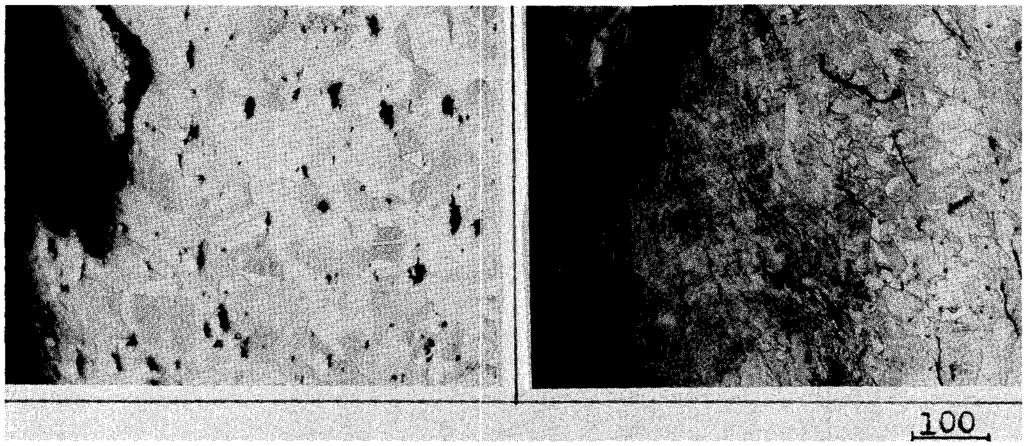

(a) COARSE G.S. (b) FINE G.S.

Fig.13. Cross section of fractured surfaces of coarse and fine grain size specimens of forged Inconel 600 in hot-torsion test.

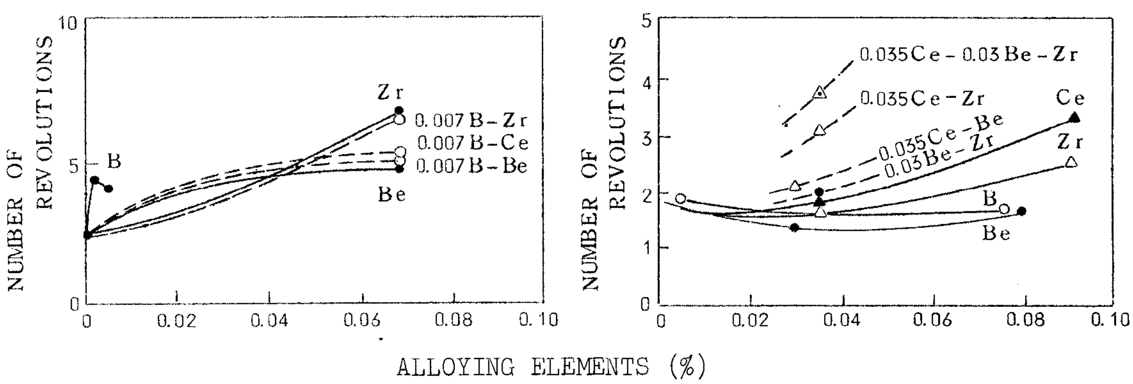

(a) Inconel 600, 1100°C (b) Hastelloy X, 1150°C

Fig.14. Effect of minor alloying elements on the hot-workability in as-casted Inconel 600 and Hastelloy X.

hot-workability.

MECHANISM
(1) Decrease of Cu and Mn content.
(2) Addition of minor elements such as B, Be, Zr, and Ce etc.
(3) Decrease of inclusions.
(4) Decrease of γ grain size.

PROCESS
(1) Electro-slag remelting.
(2) Refining at high temperature for long time under high vacuum.
(3) Diffusion-annealing under the time and temperature conditions where γ grain size does't grow too much.
(4) Increase of forging ratio.

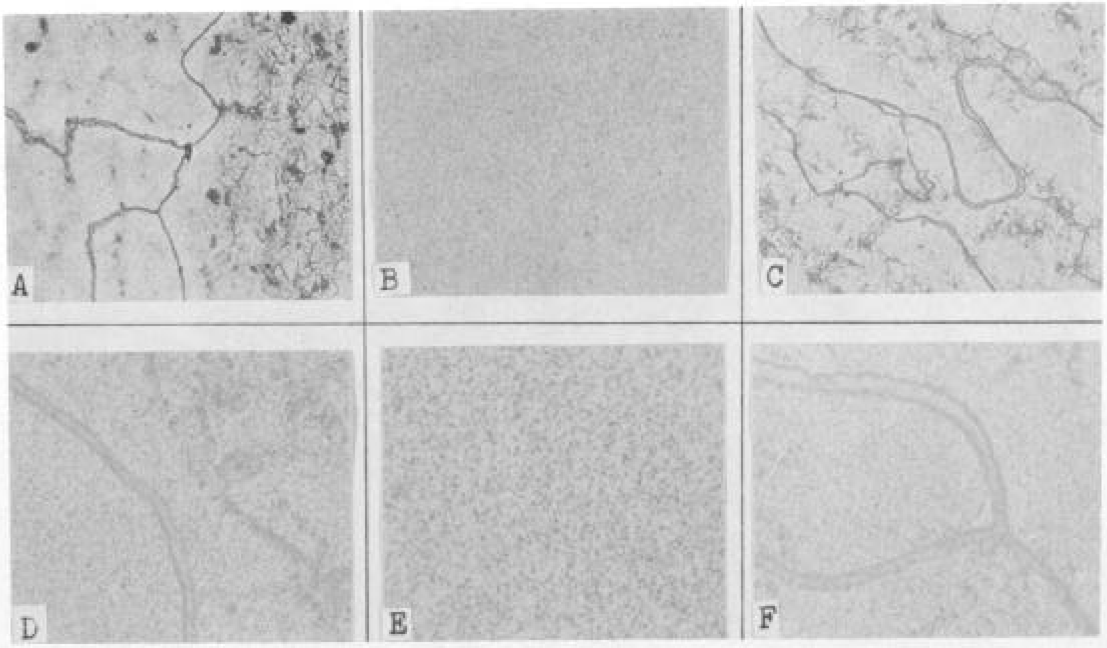

Fig.15. Distribution of B disclosed by fission track etching method in B-added Inconel 600.
A and D: B B and E: B-Be C and F: B-Zr

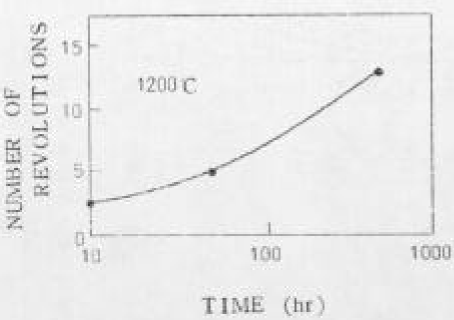

Fig.16. Effect of diffusion-annealing time at 1200°C on the hot-workability in air-melted and as-casted Inconel 600.

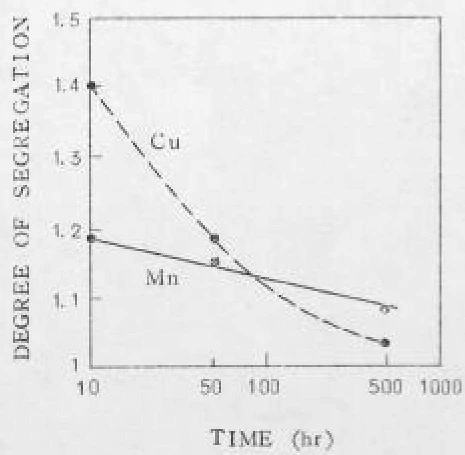

Fig.17. Effect of diffusion-annealing time at 1200°C on the segregation on γ grain boundaries.

ACKNOWLEDGEMENT

The authors are very grateful to Dr. S. Dazai, Ex-director of Research Institute for his advices and encouragements throughout the works, to Dr. Y. Nakamura for his melting practices and to Mr. A. Murota who helped us to carry out the experiments.

REFERENCES

1. The Japan Institute of Metals: Strength and Fracture of Metallic Materials (1964), p491, Maruzen

2. R. Kiessling: J. Met., 22, (1969), p48 - 52

3. ASTM: Effects of Residual Elements on Properties of Austenitic Stainless Steel. STP (1967), p418

4. E. W. Kelley: Met. Eng. Quart., p10 - 16

5. W. F. Savage and B. M. Krants: Welding J. Suppl., 50, (1971), p292 - 303

6. R. F. Decker: Steel Strengthening Mechanisms Symposium (Zurich), (1969)

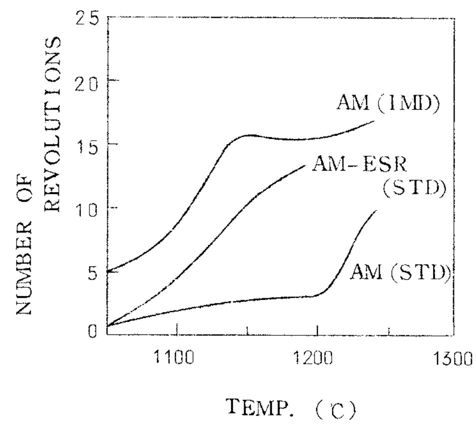

Fig.18. Hot-workability of Inconel 600 of standard composition (STD) and improved composition (IMP).